

Estimation of Soils Electrical Resistivity using Artificial Neural Network Approach

^{1,2}Kpomonè Komla Apaloo-Bara, ^{1,2}Adekunlé Akim Salami, ^{1,2}Mawugno Koffi Kodjo,
²Agbassou Guenoukpati, ²Sangué Oraléou Djandja and ^{1,2}Koffi-Sa Bedja

¹Department of Electrical Engineering, Ecole Nationale Supérieure d'Ingénieurs (ENSI), University of Lome, Togo
²Laboratoire Génie-Electrique, Ecole Nationale Supérieure d'Ingénieurs (ENSI), University of Lome, Togo

Article history

Received: 01-12-2018

Revised: 19-02-2019

Accepted: 12-03-2019

Corresponding Author:
Adekunlé Akim Salami
Department of Electrical
Engineering, Ecole Nationale
Supérieure d'Ingénieurs
ENSI, University of Lomé, Togo
Email: akim_salami@yahoo.fr

Abstract: The knowledge of the ground electrical resistivity is essential to ensure the protection of electrical and telecommunications networks. However, the monitoring of its values is an expensive task which takes long time. Therefore, its prediction is important. This study investigates on predicting soil electrical resistivity using Artificial Neural Networks. Nine sites of our city (Lome, TOGO) were considered. After characterization of the resistivity data collected on these sites, two models have been developed: Multilayer Perceptron (MLP) and Radial Basis Function (RBF) networks. Relative Root Mean Square Error (RRMSE) and R² (Linear Correlation Coefficient) have been used to evaluate each model performance. For the MLP model, the configuration [ABCDEF] is the most efficient with the RRMSE = 12.00%, R² = 81.91% and 70 neurons under the hidden layer. For the RBF model, the configuration [BCDEF] is the most efficient with the RRMSE = 16.07%, R² = 69.97% and 100 neurons under the hidden layer. In general, the results exhibit that the MLP outcome configuration [ABCDEF] is the most efficient with the best RRMSE = 16.07% and R² = 69.97%. The letter A, B and C are the weather parameters and D, E, F are the geo-referenced coordinates of the measuring point. So far, research has not focused on predicting the electrical resistivity of the soil at a given location. Thus, the results of this study show that from meteorological data, it's possible to predict this electrical resistivity.

Keywords: Characterization, Prediction, Multilayer Perceptron, Radial Basis Function, Statistics

Introduction

Electrical energy appears as the main factor for the socio-economic development of a nation. The use of this energy exposes people and property to risks. Then, leaders give themselves as a duty to protect energy networks in order to meet the ever-increasing needs of the population. One of the quality factors of this protection is the earthing system, which plays an important role in the telecommunications and power distribution networks for the safe operation of any installation (Nassereddine *et al.*, 2013; Choi and Lee, 2012; Kamel, 2011; Houndedako *et al.*, 2014; Nzuru Nsekere, 2009). Thus, a properly designed earthing system is able to dissipate large currents to the earth safely, regardless of the type of fault.

The estimation of soil electrical resistivity values is an important parameter when designing earthing

systems. The soil resistivity varies with parameters such as temperature, water content, soil composition, weather etc. It requires an adequate modeling method, this has been emphasized in (Legrand, 2007). In this regard, a classical approach has been developed to estimate soil resistance. The authors applied an Artificial Neural Networks (ANN) to the data of historical resistivity and precipitation (Asimakopoulou, 2013). Meanwhile, Dharmadasa *et al.* (2013) developed a suitable software tool with low cost to meet the requirements of the artificial intelligence concepts (Dharmadasa *et al.*, 2013).

A Generalized Neural Network Regression (GRNN) was developed to predict the soil resistance in Athens using key instabilities affecting the variation of soil resistance such as soil composition, water content, temperature, mass electrodes and electrode spacing (Anbazhagan, 2015). The study was conducted on measurements of soil resistivity, temperature and period

to estimate the variation of soil electrical resistivity throughout the year using Artificial Neural Networks (Asimakopoulou, 2011). Similar study has been performed in (Marcin and Furmanski, 2013). The authors made use of an ANN model with three hidden layers to predict thermal conductivity of granular media. The study in (Afa and Anaele, 2010) showed that seasonal variation and soil type have a considerable influence on the electrical characteristics of the soil and thus affect the performance of earth systems.

Abda et al. (2015) investigated an extreme water flow rates by help of an ANN and fuzzy inference systems against traditional statistical models in the Algerian coastal basins. The obtained results with the ANN methods have given a lower error than those obtained by the classical statistical methods.

This study focuses on modeling the soil electrical resistivity using Multilayer Perceptron and the Radial Basis Functional Networks approaches, based on the weather conditions during the measurements. It also takes into account the geo-referenced coordinates measuring point, the ambient temperature. The data were collected on nine sites of Lome city (Togo). These sites are West side of Institut Confucius, North side of Institut Confucius, West side of Institut Confucius, South side of Campus numérique, North side of Campus numérique, West side of Campus numérique, South side of Bloc Pédagogique, North side of Bloc Pédagogique and West side of Bloc Pédagogique. These sites were chosen due to the need of improving the electrical protection system and the safety of goods, people against electrical defects.

Study Models

In principle, ANN can be applied to perform many tasks, such as pattern recognition or classification problems, (Gronarz et al., 2016). In our present investigation, their capability for function approximation and interpolation is used.

The output of a neural network takes into account the learning procedure. The learning process is based on the retro propagation of the error. Its output is expressed as shown by relation (1):

$$O_k = \sum_{j=1}^q W_{kj} b_j(x) - \theta_k \quad (1)$$

Where:

- $1 < k < m$; m = The number of nodes
- O_k = The output of the k_{th} node of the output layer
- W_{kj} = The connection between the j_{th} neuron of hidden layer and k_{th} neuron of output layer
- $b_j(x)$ = The output of the j_{th} neuron of the hidden layer
- θ_k = The bias of the k_{th} neuron of output layer

The architecture of Multilayer Perceptron (MLP) model is shown in Fig. 1. The output of this model is given by relation (2):

$$y = \beta_0 + \sum_{i=1}^n \beta_i h_i \quad (2)$$

Where:

y = The predicted value with the neural network

n = The number of hidden layers

β_0 = The bias

β_i = The weighted coefficients

h_i = The result of the non-linear transformation of the i^{th} hidden unit

The basic radial function model (RBF) differs from the MLP model by a Gaussian activation function at the hidden layer as shown in Fig. 2. During the learning process, each neuron in the hidden layer performs a nonlinear transformation (Akim Salami et al., 2018). The output of the model is expressed as follows by the relation (3):

$$b_j(X) = \exp \left[-\frac{\sum_{i=1}^n (X_i - \mu_j)^2}{2\sigma_j^2} \right] \quad (3)$$

Where:

μ_j and σ_j = Respectively the center and the width (standard deviation) of the Gaussian function of the j_{th} neuron of the hidden layer

X_i = Input variables of the neuron

q = The number of neurons in the hidden layer ($1 \leq j \leq q$)

Four indicators are taken into account in the evaluation of the performances of the various configurations: Mean Absolute Percentage Error (MAPE), Root Mean Square Error (RMSE), Relative Root Mean Square Error (RRMSE) and the correlation coefficient (R^2). These indicators are given by the relations (4 to 7):

$$MAPE = \frac{1}{N} \left| \frac{Y_{j,p} - Y_{j,r}}{Y_{j,r}} \right| \times 100 \quad (4)$$

$$PMSE = \sqrt{\frac{1}{N} \sum_{j=1}^N (Y_{j,p} - Y_{j,r})^2} \quad (5)$$

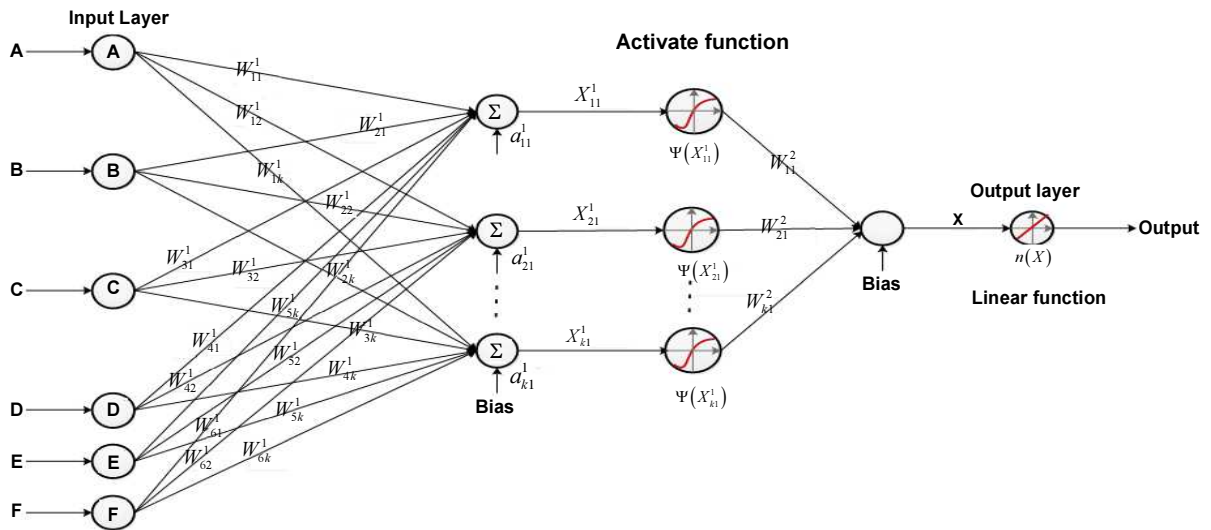


Fig. 1: Neural architecture of the MLP model

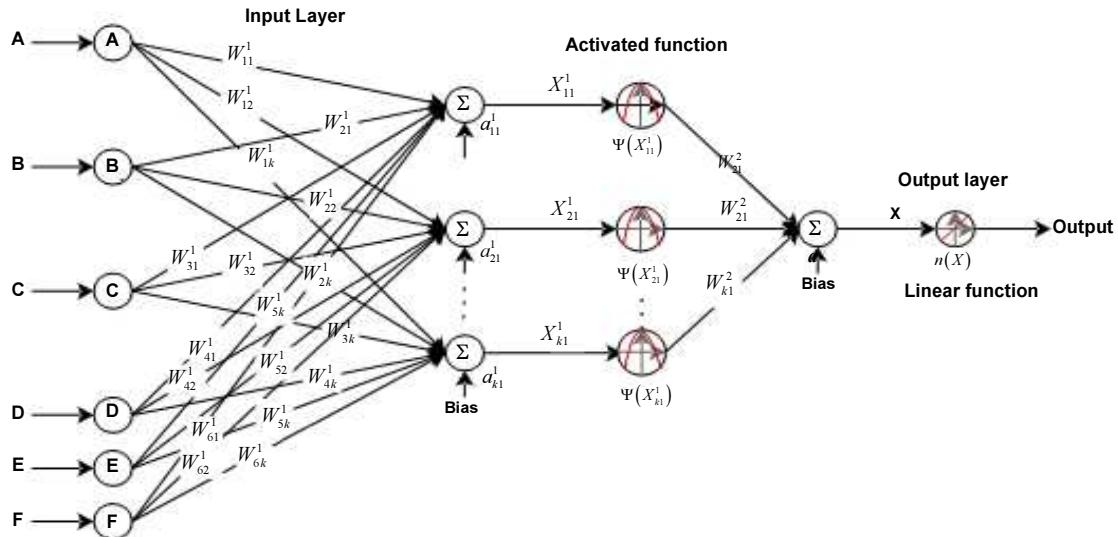


Fig. 2: Neural architecture of the RBF model

$$RRMSE = \sqrt{\frac{\frac{1}{N} \sum_{j=1}^N (Y_{j,p} - Y_{j,r})^2}{\frac{1}{N} \sum_{j=1}^N Y_{j,r}}} \quad (6)$$

$$R^2 = \frac{\sum_{j=1}^N (Y_{j,p} - Y_{p,avg}) \times (Y_{j,r} - Y_{p,avg})}{\sqrt{\left[\sum_{j=1}^N (Y_{j,p} - Y_{p,avg})^2 \right] \times \left[\sum_{j=1}^N (Y_{j,r} - Y_{p,avg})^2 \right]}} \quad (7)$$

In relations (4), (5), (6) and (7), N is the number of measured values; $Y_{j,p}$ are the estimated values; $Y_{j,r}$ are measured values; $Y_{p,avg}$ is the predicted mean value and $Y_{r,avg}$ is the measured mean value.

Methodology

The Data processing and implementation of the prediction models were performed using the "nftool" toolbox of the Matlab software. The data used come from the Wenner method (Wenner, 1915), with electrodes embedded in the ground to a depth of one metre (1 m) on the nine (09) sites whose geo-referenced coordinates are presented in Table 1. Pre-treatment was

carried out to reduce noise. In order to get an idea of the evolution of the resistivity data on each site, a characterization was made according to the different explanatory parameters. For forecasting work, the data are classified into two groups. The first learning group consists of data from the seven (07) sites. The second

group uses data from the two (02) remaining sites to validate the effectiveness of the forecast. The measured data are preprocessed to make them usable by the software. The coding of the four input variables used and all their possible combinations are respectively presented in Tables 2 and 3.

Table 1: Geo-referenced coordinates

Site	Name of the site	Geographical Position	Polar Coordinates
Site 1	South side of Institut Confucius	North Latitude	06°10.392
		East longitude	001°12.699
		Altitude	38 m
Site 2	North side of Institut Confucius	North Latitude	06°10.397
		East longitude	001°12.698
		Altitude	38 m
Site 3	West side of Institut Confucius	North Latitude	06°10.395
		East longitude	001°12.706
		Altitude	38 m
Site 4	South side of Campus numérique	North Latitude	06°10.176
		East longitude	001°12.731
		Altitude	33 m
Site 5	North side of Campus numérique	North Latitude	006°10.818
		East longitude	001°12.732
		Altitude	35 m
Site 6	West side of Campus numérique	North Latitude	06°10.180
		East longitude	001°12.736
		Altitude	35 m
Site 7	South side of Bloc Pedagogique	North Latitude	06°10.423
		East longitude	001°12.845
		Altitude	30 m
Site 8	North side of Bloc Pédagogique	North Latitude	06°10.429
		East longitude	001°12.842
		Altitude	32 m
Site 9	West side of Bloc Pédagogique	North Latitude	06°10.432
		East longitude	001°12.847
		Altitude	31 m

Table 2: Explanatory variables

Input variables	Mathematical explanation	Code
State of nature during the day of measurement	Less sunny = 1; Very Sunny = 2; Sunny = 3; Cloudy = 4; Rainy = 5; Partially covered = 6	A
State of nature during the previous day	Less sunny = 1; Very Sunny = 2; Sunny = 3; Cloudy = 4; Rainy = 5; Partially covered = 6	B
Ambient temperature (in ° C) at the measuring point	25 to 35.	C
Longitude	-	D
Latitude	-	E
Altitude	-	F

Table 3: List of possible configuration

Number	Configuration
1	[AB]
2	[AC]
3	[AD]
4	[BC]
5	[BDEF]
6	[CDEF]
7	[ABC]
8	[ABDEF]
9	[ACDEF]
10	[BCDEF]
11	[ABCDEF]

After this step, we choose the model for the learning phase. The accuracy of the model may depend on the choice of input parameters. This involves the elimination of some redundant variables those provide less or no information to describe the output. Thus we explore all the configurations for each of the two models in order to retain the one that will provide the smallest error (RRMSE). The diagram in Fig. 3 summarizes the entire survey.

Results

Table 4 shows the statistical parameters of the measured resistivity data. frequency histograms superimposed on the normal distribution function are showed for each site in Figs. 4, 5, 6, 7, 8, 9, 10, 11 and 12. Fig. 13 gives information between resistivity classes and the ambient temperature. For prediction, the number of hidden layer neurons and performance indicators are given for both models, the MLP and the RBF.

Table 4: Statistical characteristics of the resistivity data

Site	Mean	Standard deviation	Minimum	Maximum	Mode	Median	Kurtosis	Skewness
Site 1	172.839	19.721	88.542	235.569	188.496	174.078	3.257	-0.379
Site 2	89.868	17.943	35.801	155.938	82.015	90.408	3.077	0.097
Site 3	132.309	21.167	65.681	216.882	65.681	132.268	3.162	0.119
Site 4	139.708	21.926	61.378	217.960	157.080	140.651	3.187	-0.159
Site 5	103.150	17.577	24.600	221.334	125.664	102.097	6.028	0.477
Site 6	192.506	20.188	126.515	282.535	219.912	191.784	3.455	0.044
Site 7	188.459	14.320	133.833	240.727	188.496	188.496	3.922	-0.125
Site 8	122.328	13.244	83.898	168.515	125.664	122.296	3.067	0.092
Site 9	177.272	18.711	102.917	244.794	188.496	177.580	3.082	-0.001

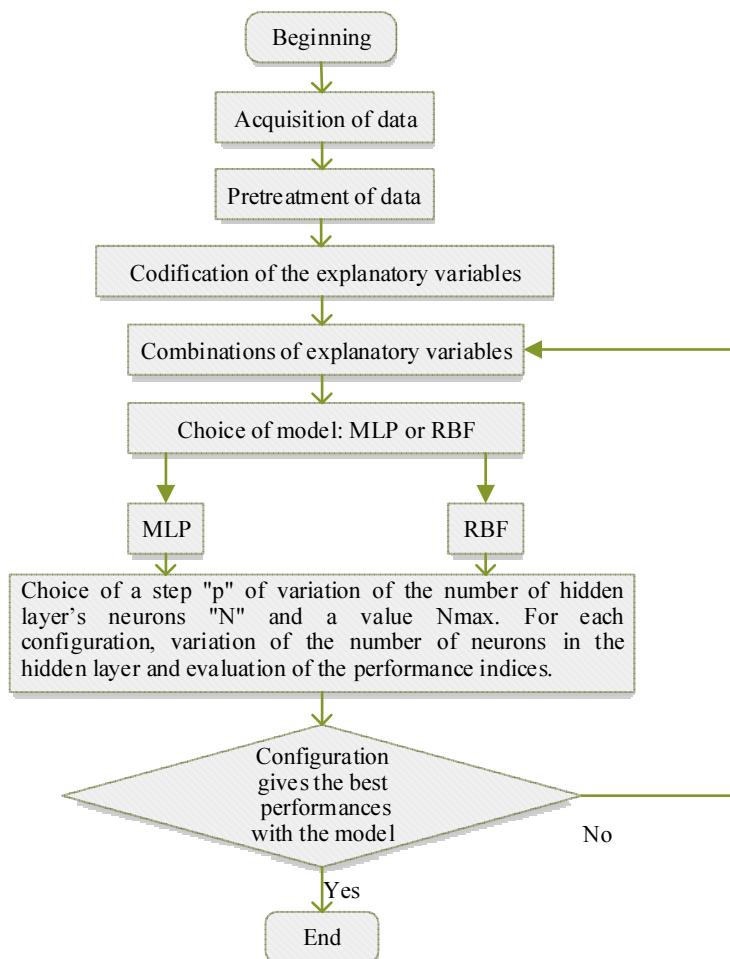


Fig. 3: Methodology adopted for the prediction of the soil electrical resistivity

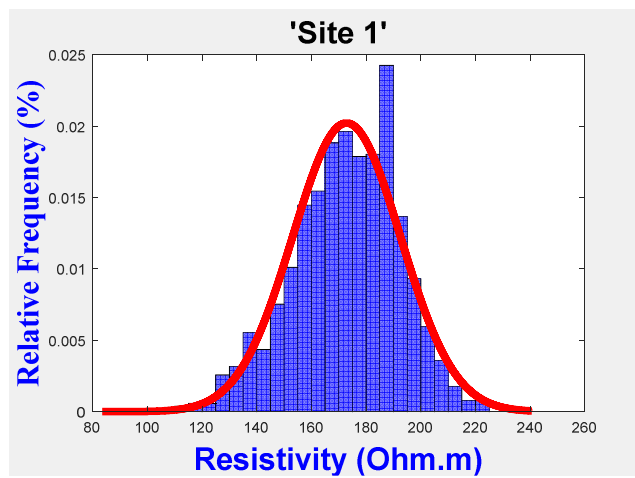


Fig. 4: Distribution of resistivity data for site 1

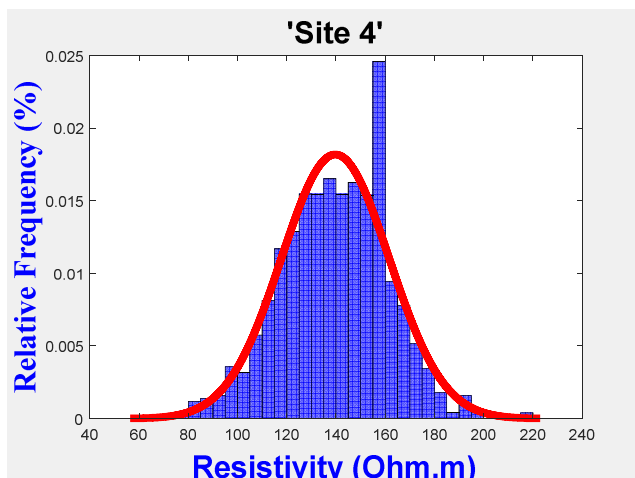


Fig. 7: Distribution of resistivity data for site 4

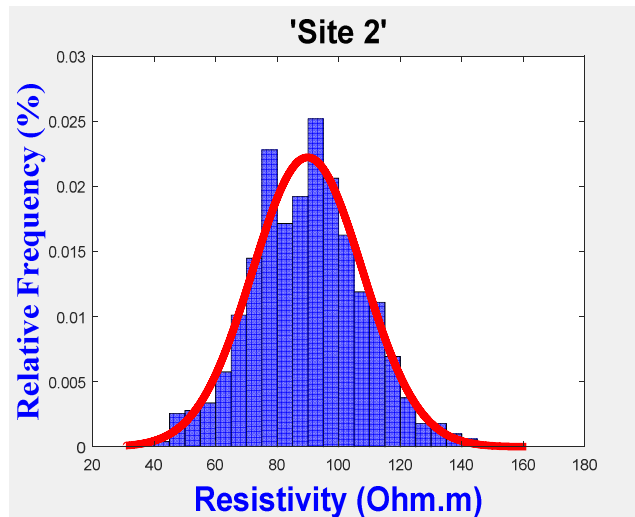


Fig. 5: Distribution of resistivity data for site 2

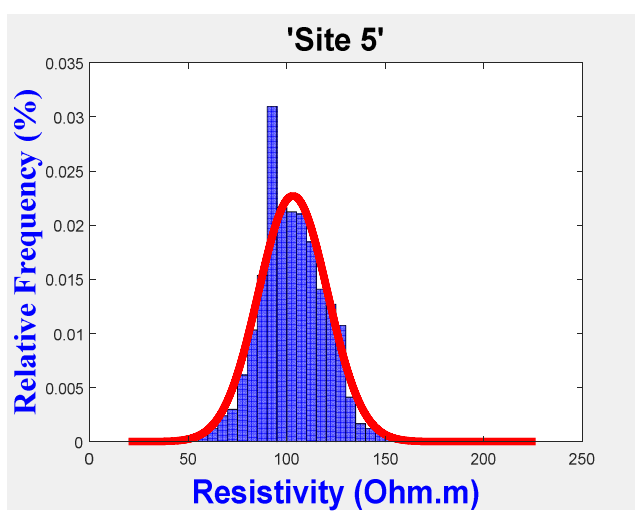


Fig. 8: Distribution of resistivity data for site 5

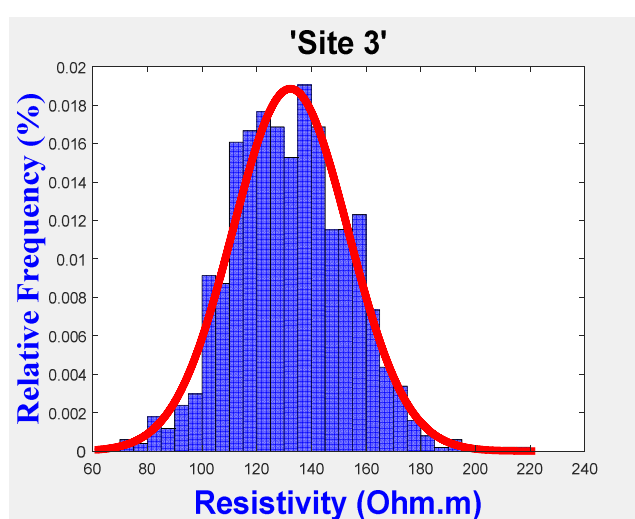


Fig. 6: Distribution of resistivity data for site 3

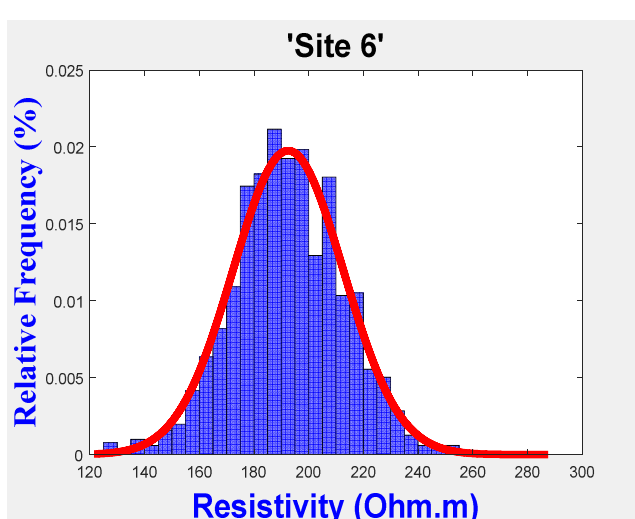


Fig. 9: Distribution of resistivity data for site 6

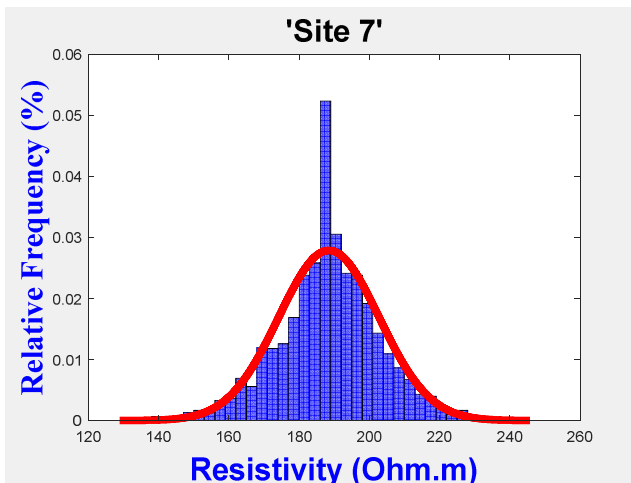


Fig. 10: Distribution of resistivity data for site 7

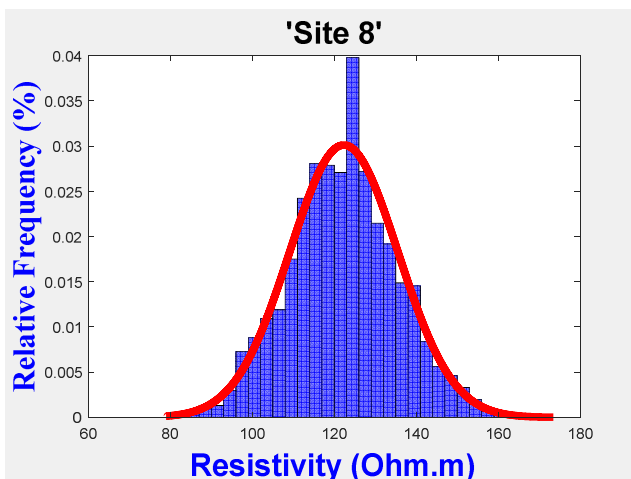


Fig. 11: Distribution of resistivity data for site 8

For each of these models, ten learning configurations are considered in the simulation as shown in Tables 5 to 15 and 16 to 26, respectively for MLP and RBF. In these tables, the symbol (*) and in bold indicates the best performance of a given configuration. Indeed, the synaptic weights change with each run, which introduces a slight difference in the results at each iteration.

Table 27 summarizes the performance of all configurations for the two models considered with respect to the defined number of neurons for the hidden layer and performance indicators.

Discussion

The coefficients of "Kurtosis" and "Skewness" of the measured resistivity data showed in Table 4, led to the conclusion that the evolution of the resistivity data is close to the normal distribution. To confirm that "Normal" aspect of the data, frequency histograms were superimposed on the normal distribution function.

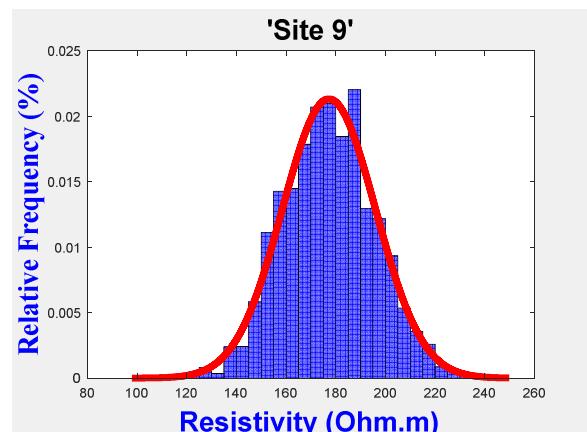


Fig. 12: Distribution of resistivity data for site 9

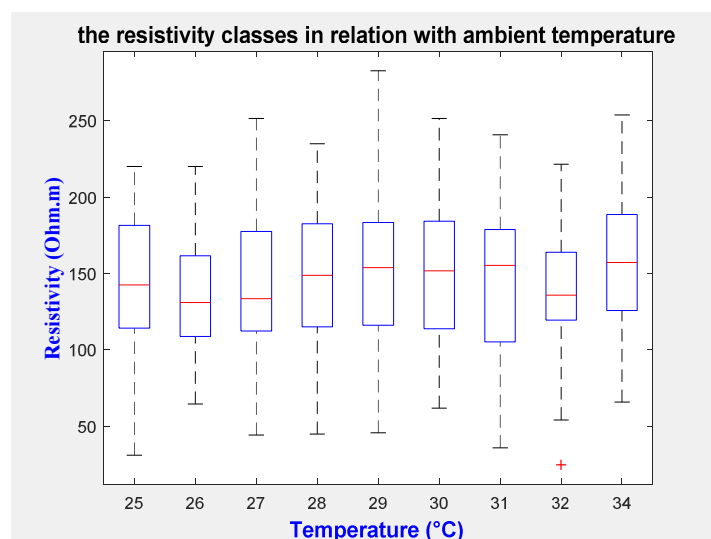


Fig. 13: Soil resistivity classes according to ambient temperature

Table 5: MLP model performances - configuration “1“(AB])

Number of hidden layer's neurons	RMSE		RRMSE (%)		MAPE (%)		R ² (%)	
	Min	Max	Min	Max	Min	Max	Min	Max
1	39.8442	39.9731	28.1362	28.2273	28.4638	28.9513	0.0894	0.5787
5	39.5184	39.8790	27.9062	28.1608	28.0885	28.6337	0.4294	2.1987
10	39.4690	39.6762	27.8713	28.0176	28.0322	28.6427	1.6645	2.4479
20	39.4599	39.6390	27.8649	27.9913	28.0021	28.2687	1.8310	2.4914
30	39.4622	39.7213	27.8665	28.0495	27.9944	28.4081	1.4669	2.4798
40	39.4602	39.4878	27.8651	27.8845	28.0784	28.3045	2.3868	2.4895
60	39.4594	39.7541	27.8645	28.0726	28.1086	28.2625	1.6189	2.4884
70	39.4590	39.7860	27.8642	28.0952	28.0237	28.2560	1.5938	2.4924
80*	39.4579	39.4812	27.8635	27.8799	28.0635	28.2730	2.3864	2.4955
90	39.4600	39.5711	27.8650	27.9434	28.0566	28.2008	2.0387	2.4998
100	39.4611	39.4776	27.8657	27.8774	28.0467	28.2106	2.4076	2.4914

Table 6: MLP model performances - configuration “2“(AC])

Number of hidden layer's neurons	RMSE		RRMSE (%)		MAPE (%)		R ² (%)	
	Min	Max	Min	Max	Min	Max	Min	Max
1	39.7797	39.8773	28.0907	28.1596	28.3000	28.6605	0.5719	0.9003
5	39.5154	39.7831	27.9041	28.0931	28.2415	28.5467	0.8816	2.2121
10	39.4366	39.6674	27.8484	28.0114	28.1288	28.4177	1.4833	2.6183
20	39.4256	39.7117	27.8406	28.0427	27.9646	28.5095	1.4841	2.6577
30	39.4240	39.5577	27.8395	27.9339	27.7419	28.1967	2.3752	2.6636
40	39.4229	39.4976	27.8388	27.8915	27.9922	28.1998	2.3959	2.6679
60	39.4235	39.6325	27.8392	27.9868	28.0901	28.2697	1.9444	2.6670
70*	39.4228	39.4416	27.8387	27.8519	28.1111	28.2423	2.5781	2.6712
80	39.4241	39.4412	27.8396	27.8517	28.0569	28.2404	2.5951	2.6660
90	39.4255	39.4417	27.8406	27.8520	28.0770	28.2588	2.5843	2.6610
100	39.4239	39.4536	27.8395	27.8604	28.0587	28.2231	2.5393	2.6740

Table 7: MLP model performances - configuration “3“(ADEF])

Number of hidden layer's neurons	RMSE		RRMSE(%)		MAPE (%)		R ² (%)	
	Min	Max	Min	Max	Min	Max	Min	Max
1	36.5449	39.8971	25.8064	28.1736	25.1170	28.5142	0.3214	16.3603
5	17.5809	34.0620	12.4149	24.0531	10.8695	22.7493	27.3407	80.6446
10	17.4551	21.0639	12.3261	14.8744	10.7484	12.6994	72.2216	80.9202
20	17.4433	18.1469	12.3177	12.8146	10.7453	11.0941	79.3766	80.9452
30	17.4418	17.4560	12.3167	12.3267	10.7399	10.8076	80.9189	80.9495
40*	17.4412	17.4561	12.3162	12.3268	10.7430	10.7881	80.9170	80.9495
60	17.4409	17.4888	12.3160	12.3498	10.7366	10.8289	80.8497	80.9502
70	17.4429	17.5152	12.3174	12.3685	10.7476	10.8039	80.7971	80.9461
80	17.4421	17.4607	12.3168	12.3300	10.7492	10.7939	80.9092	80.9489
90	17.4435	17.4706	12.3179	12.3370	10.7341	10.7926	80.9072	80.9462
100	17.4418	17.4621	12.3166	12.3310	10.7516	10.7933	80.9042	80.9482

Table 8: MLP model performances- configuration “4“(BC])

Number of hidden layer's neurons	RMSE		RRMSE (%)		MAPE (%)		R ² (%)	
	Min	Max	Min	Max	Min	Max	Min	Max
1	39.7616	39.9597	28.0779	28.2178	28.2439	28.7484	0.0000	0.9958
5	39.5252	39.8777	27.9110	28.1599	28.0995	29.0465	0.8896	2.1694
10	39.4669	39.6788	27.8698	28.0195	27.9650	28.4044	1.4212	2.4548
20	39.4506	39.6723	27.8583	28.0149	27.9928	28.2584	1.7406	2.5396
30	39.4478	39.5728	27.8563	27.9446	28.0538	28.4207	2.0655	2.5461
40	39.4486	39.8551	27.8569	28.1440	28.0458	28.2541	1.8231	2.5439
60	39.4505	39.4719	27.8582	27.8733	28.0663	28.2786	2.4459	2.5394
70*	39.4527	39.4688	27.8598	27.8711	28.0220	28.2038	2.4429	2.5292
80	39.4482	39.5688	27.8566	27.9417	28.0414	28.3147	2.0862	2.5444
90	39.4498	39.4737	27.8578	27.8746	28.0761	28.2349	2.4189	2.5400
100	39.4491	39.8358	27.8572	28.1303	28.0461	28.2532	1.4698	2.5390

Table 9: MLP model performances - configuration “5“([BDEF])

Number of hidden layer's neurons	RMSE		RRMSE (%)		MAPE (%)		R ² (%)	
	Min	Max	Min	Max	Min	Max	Min	Max
1	36.5452	39.9598	25.8066	28.2179	25.1337	28.6714	0.0000	16.3598
5	17.7001	33.4190	12.4991	23.5990	10.9796	21.8946	30.0576	80.3807
10	17.6618	21.9858	12.4720	15.5254	10.9278	13.2188	69.7301	80.4655
20	17.6592	20.2096	12.4702	14.2711	10.9289	12.3863	74.4237	80.4714
30	17.6569	18.0080	12.4685	12.7164	10.9249	11.0014	79.6938	80.4753
40	17.6584	18.5181	12.4696	13.0766	10.9059	11.0267	78.5605	80.4733
60	17.6566	17.9732	12.4683	12.6919	10.9268	11.0218	79.7786	80.4767
70*	17.6568	17.7824	12.4685	12.5571	10.9292	10.9960	80.1969	80.4757
80	17.6577	18.1055	12.4691	12.7853	10.9211	11.0094	79.4760	80.4738
90	17.6583	19.1451	12.4695	13.5195	10.9155	11.0234	77.1712	80.4726
100	17.6570	18.4004	12.4686	12.9936	10.9291	10.9946	78.8256	80.4751

Table 10: MLP model performances - configuration “6“([CDEF])

Number of hidden layer's neurons	RMSE		RRMSE (%)		MAPE (%)		R ² (%)	
	Min	Max	Min	Max	Min	Max	Min	Max
1	36.4996	39.5643	25.7745	27.9386	25.0207	28.3850	1.9753	16.5683
5	17.3300	25.5487	12.2377	18.0414	10.6441	15.7790	59.1220	81.1914
10	16.9756	17.3841	11.9874	12.2759	10.3792	10.7569	81.0744	81.9534
20	16.8622	17.0977	11.9073	12.0736	10.2154	10.5263	81.6964	82.1946
30	16.8560	16.8890	11.9030	11.9263	10.1726	10.2884	82.1400	82.2069
40	16.8538	16.8781	11.9015	11.9186	10.1814	10.2451	82.1645	82.2114
60	16.8557	16.9897	11.9028	11.9974	10.1740	10.4274	81.9522	82.2077
70	16.8543	16.8779	11.9018	11.9184	10.1729	10.2085	82.1602	82.2099
80	16.8539	16.8855	11.9015	11.9238	10.1763	10.2269	82.1513	82.2113
90	16.8565	16.8752	11.9033	11.9166	10.1591	10.2296	82.1678	82.2057
100*	16.8572	16.8701	11.9039	11.9129	10.1833	10.2210	82.1777	82.2055

Table 11: MLP model performances - configuration “7“([ABC])

Number of hidden layer's neurons	RMSE		RRMSE (%)		MAPE (%)		R ² (%)	
	Min	Max	Min	Max	Min	Max	Min	Max
1	39.7235	39.7626	28.0510	28.0786	28.2722	28.4985	0.9966	1.1781
5	39.4224	39.7390	27.8384	28.0620	28.0818	28.4754	1.1044	2.6772
10	39.1153	39.6192	27.6215	27.9773	27.8465	28.3227	1.6970	4.1816
20	38.9951	39.4690	27.5366	27.8713	27.6229	28.4488	2.6882	4.8050
30	38.9629	39.1964	27.5139	27.6788	27.5836	28.0378	3.8610	4.9463
40	38.9525	39.0829	27.5065	27.5987	27.6477	27.8575	4.3713	4.9772
60	38.9489	39.0208	27.5041	27.5548	27.5828	27.8232	4.6897	5.0488
70*	38.9510	39.0063	27.5055	27.5446	27.6195	27.7830	4.7271	4.9850
80	38.9511	39.1495	27.5056	27.6457	27.4736	27.8621	4.2574	5.0005
90	38.9590	39.0139	27.5111	27.5499	27.5975	27.9089	4.7423	4.9759
100	38.9504	39.1236	27.5051	27.6274	27.5230	28.1248	4.4118	5.0251

Table 12: MLP model performances - configuration “8“([ABDEF])

Number of hidden layer's neurons	RMSE		RRMSE (%)		MAPE (%)		R ² (%)	
	Min	Max	Min	Max	Min	Max	Min	Max
1	36.5422	39.4970	25.8045	27.8911	25.0628	27.9664	2.3075	16.3732
5	17.5557	35.2510	12.3971	24.8927	10.8580	24.1873	22.1834	80.7010
10	17.4248	26.8696	12.3046	18.9741	10.7460	16.7680	54.7873	80.9857
20	17.3234	17.4490	12.2331	12.3217	10.6383	10.8183	80.9336	81.2066
30	17.2853	17.4708	12.2061	12.3371	10.6123	10.8197	80.9001	81.2901
40	17.2470	17.6561	12.1791	12.4680	10.5905	10.7853	80.4864	81.3718
60*	17.2371	17.3641	12.1721	12.2618	10.5625	10.6200	81.1186	81.3949
70	17.2284	17.6750	12.1660	12.4813	10.5535	10.7838	80.4468	81.4121
80	17.2276	17.4972	12.1654	12.3558	10.5436	10.6300	80.8325	81.4135
90	17.2312	17.9114	12.1680	12.6482	10.5673	10.6421	79.9316	81.4052
100	17.2317	18.9791	12.1682	13.4022	10.5480	10.6546	77.6163	81.4077

Table 13: MLP model performances - configuration “9“([ACDEF])

Number of hidden layer's neurons	RMSE		RRMSE (%)		MAPE (%)		R ² (%)	
	Min	Max	Min	Max	Min	Max	Min	Max
1	36.4996	39.8456	25.7744	28.1372	24.9983	28.5002	0.5696	16.5690
5	17.3731	31.4688	12.2681	22.2219	10.6970	20.1873	37.9893	81.0990
10	17.1013	17.4215	12.0762	12.3023	10.4876	10.7287	80.9937	81.6853
20	16.9494	18.6242	11.9690	13.1516	10.3567	11.3429	78.2787	82.0091
30	16.8386	17.1984	11.8907	12.1448	10.2432	10.6045	81.4895	82.2433
40	16.7878	17.0220	11.8548	12.0202	10.1696	10.4267	81.8548	82.3520
60	16.7494	16.9467	11.8277	11.9670	10.1008	10.3013	82.0224	82.4337
70	16.7554	16.8926	11.8320	11.9289	10.0998	10.3576	82.1347	82.4217
80	16.7487	16.8257	11.8272	11.8816	10.0871	10.2098	82.3093	82.4325
90	16.7503	16.7930	11.8283	11.8585	10.0895	10.1979	82.3442	82.4305
100*	16.7465	16.7860	11.8257	11.8536	10.1005	10.1583	82.3541	82.4367

Table 14: MLP model performances - configuration “10“([BCDEF])

Number of hidden layer's neurons	RMSE		RRMSE (%)		MAPE (%)		R ² (%)	
	Min	Max	Min	Max	Min	Max	Min	Max
1	36.4982	39.9696	25.7734	28.2248	24.9701	28.8340	0.0000	16.5768
5	17.3229	27.4144	12.2327	19.3588	10.6355	16.7436	52.9372	81.2094
10	17.0115	31.1832	12.0128	22.0202	10.4249	19.8923	39.1041	81.8767
20	16.8975	17.2542	11.9323	12.1842	10.3187	10.6228	81.3567	82.1205
30	16.8080	17.6977	11.8691	12.4973	10.2212	10.6426	80.3882	82.3075
40*	16.7759	17.0410	11.8464	12.0336	10.1469	10.5324	81.8225	82.3784
60	16.7548	18.1900	11.8315	12.8450	10.1094	10.3823	79.3795	82.4222
70	16.7438	17.7079	11.8237	12.5046	10.0945	10.8893	80.6711	82.4427
80	16.7432	18.6552	11.8233	13.1735	10.0959	11.3790	78.4185	82.4441
90	16.7493	17.3609	11.8276	12.2595	10.0938	10.1927	81.1445	82.4311
100	16.7391	17.7650	11.8204	12.5448	10.0886	10.6405	80.3400	82.4546

Table 15: MLP model performances - configuration “11“([ABCDEF])

Number of hidden layer's neurons	RMSE		RRMSE (%)		MAPE (%)		R ² (%)	
	Min	Max	Min	Max	Min	Max	Min	Max
1	36.4977	39.8827	25.7731	28.1634	24.9882	28.5518	0.9919	16.5765
5	17.3266	35.2290	12.2353	24.8772	10.6478	24.0076	22.2770	81.1994
10	17.0921	32.4941	12.0697	22.9459	10.4648	21.2098	33.8770	81.7045
20	16.9263	25.6483	11.9526	18.1117	10.3242	15.7694	58.8051	82.0582
30	16.8525	17.1536	11.9005	12.1131	10.3006	10.5025	81.5779	82.2150
40	16.8976	17.2246	11.9323	12.1632	10.3282	10.5878	81.4253	82.1214
60	16.7154	17.0286	11.8037	12.0249	10.1114	10.4429	81.8402	82.5029
70*	16.7208	16.9969	11.8075	12.0025	10.1373	01.4131	81.9100	82.4912
80	16.6731	17.0044	11.7738	12.0077	10.0973	10.4823	81.9225	82.5906
90	16.6195	17.0389	11.7360	12.0321	10.0157	10.4490	81.8397	82.7044
100	16.5777	17.0149	11.7064	12.0152	9.9629	10.5049	81.9149	82.7896

Table 16: RBF model performances - configuration “1“([AB])

Number of hidden layer's neurons	RMSE		RRMSE (%)		MAPE (%)		R ² (%)	
	Min	Max	Min	Max	Min	Max	Min	Max
1	39.7618	39.8940	28.0780	28.1714	28.4343	28.5519	0.3278	0.9875
5	39.5395	39.8430	27.9211	28.1354	28.2374	28.4977	0.5829	2.1086
10	39.5037	39.8228	27.8958	28.1211	28.1748	28.4776	0.6837	2.2868
20	39.4603	39.5934	27.8652	27.9591	28.1423	28.2677	1.8250	2.4836
30	39.4514	39.5236	27.8588	27.9098	28.1341	28.2080	2.1712	2.5274
40	39.4513	39.4860	27.8588	27.8833	28.1380	28.1843	2.3560	2.5275
60	39.4513	39.4594	27.8588	27.8645	28.1388	28.1474	2.4879	2.5275
70	39.4513	39.4593	27.8588	27.8645	28.1388	28.1474	2.4881	2.5275
80	39.4513	39.4593	27.8588	27.8645	28.1388	28.1474	2.4881	2.5275
90*	39.4513	39.4593	27.8588	27.8645	28.1388	28.1474	2.4881	2.5275
100	39.4513	39.4593	27.8588	27.8645	28.1388	28.1474	2.4881	2.5275

Table 17: RBF model performances - configuration “2“([AC])

Number of hidden layer's neurons	RMSE		RRMSE (%)		MAPE (%)		R ² (%)	
	Min	Max	Min	Max	Min	Max	Min	Max
1	39.8003	39.8003	28.1052	28.1052	28.4715	28.4850	0.7957	0.7964
5	39.6672	39.7199	28.0113	28.0485	28.3761	28.4460	1.1999	1.4673
10	39.5517	39.6930	27.9297	28.0295	28.2951	28.4102	1.3360	2.0671
20	39.5267	39.7008	27.9121	28.0350	28.2741	28.4119	1.3320	2.1780
30	39.4262	39.6398	27.8411	27.9919	28.1340	28.3746	1.6055	2.6528
40	39.4131	39.6279	27.8318	27.9835	28.1586	28.3553	1.6593	2.7164
60	39.4131	39.6264	27.8318	27.9824	28.1566	28.3289	1.6783	2.7164
70	39.4131	39.6234	27.8318	27.9803	28.1586	28.3288	1.6893	2.7164
80*	39.4131	39.5789	27.8318	27.9489	28.1586	28.3248	1.9281	2.7164
90	39.4131	39.6110	27.8318	27.9715	28.1586	28.3347	1.7426	2.7164
100	39.4131	39.5949	27.8318	27.9602	28.1586	28.3343	1.8356	2.7164

Table 18: RBF model performances - configuration “3“([ADEF])

Number of hidden layer's neurons	RMSE		RRMSE (%)		MAPE (%)		R ² (%)	
	Min	Max	Min	Max	Min	Max	Min	Max
1	38.4674	38.4674	27.1640	27.1640	26.8978	26.8978	7.3291	7.3291
5	34.4076	34.4076	24.2971	24.2971	23.2587	23.2587	27.4259	27.4259
10	33.9576	33.9576	23.9794	23.9794	23.1284	23.1284	29.8948	29.8948
20	30.4604	30.4604	21.5098	21.5098	19.9214	19.9214	44.7656	44.7656
30	21.8054	21.8054	15.3980	15.3980	13.2989	13.2989	71.0776	71.0776
40	19.2551	19.2551	13.5971	13.5971	11.8260	11.8260	76.9093	76.9093
60	17.4350	17.4350	12.3118	12.3118	10.7610	10.7610	80.9628	80.9628
70*	17.4350	17.4350	12.3118	12.3118	10.7608	10.7608	80.9628	80.9628
80	17.4350	17.4350	12.3118	12.3118	10.7607	10.7607	80.9628	80.9628
90	17.4350	17.4350	12.3118	12.3118	10.7610	10.7610	80.9628	80.9628
100	17.4350	17.4350	12.3118	12.3118	10.7608	10.7608	80.9628	80.9628
30	21.8054	21.8054	15.3980	15.3980	13.2989	13.2989	71.0776	71.0776

Table 19: RBF model performances - configuration “4“([BC])

Number of hidden layer's neurons	RMSE		RRMSE (%)		MAPE (%)		R ² (%)	
	Min	Max	Min	Max	Min	Max	Min	Max
1	39.7433	39.7570	28.0650	28.0747	28.3934	28.4005	1.0112	1.0793
5	39.5423	39.6735	27.9231	28.0157	28.2160	28.3281	1.4266	2.0922
10	39.5151	39.6735	27.9038	28.0157	28.1921	28.3282	1.4266	2.2223
20	39.4531	39.5995	27.8600	27.9634	28.1428	28.2797	1.7941	2.5206
30	39.4455	39.5663	27.8547	27.9400	28.1440	28.2253	1.9719	2.5564
40	39.4404	39.5388	27.8511	27.9206	28.1400	28.2307	2.0952	2.5820
60	39.4387	39.4921	27.8499	27.8876	28.1392	28.1857	2.3261	2.5901
70	39.4387	39.4864	27.8499	27.8836	28.1417	28.1789	2.3542	2.5901
80	39.4387	39.4864	27.8499	27.8836	28.1417	28.1789	2.3542	2.5901
90	39.4387	39.4864	27.8499	27.8836	28.1417	28.1789	2.3542	2.5901
100*	39.4387	39.4864	27.8499	27.8836	28.1417	28.1789	2.3542	2.5901

Table 20: RBF model performances - configuration “5“([BDEF])

Number of hidden layer's neurons	RMSE		RRMSE (%)		MAPE (%)		R ² (%)	
	Min	Max	Min	Max	Min	Max	Min	Max
1	37.8621	38.3356	26.7366	27.0709	26.7304	26.8668	7.9629	10.2222
5	25.6990	37.5704	18.1475	26.5306	15.7510	26.5779	11.6630	58.6508
10	24.3985	35.1885	17.2292	24.8486	15.6374	24.3738	25.1413	63.2369
20	17.6683	36.4971	12.4766	25.7727	10.9535	24.9190	18.1808	80.4499
30	17.6568	36.5629	12.4685	25.8192	10.9432	25.5233	20.7757	80.4753
40	17.6527	35.7994	12.4656	25.2800	10.9401	25.6907	23.4287	80.4845
60	17.6539	35.8365	12.4664	25.3062	10.9412	25.7335	23.3325	80.4818
70	17.6527	35.9993	12.4656	25.4212	10.9398	25.6987	21.8116	80.4845
80	17.6527	36.0647	12.4656	25.4673	10.9398	25.7698	21.4940	80.4845
90*	17.6527	33.8514	12.4656	23.9044	10.9398	23.9074	34.7432	80.4845
100	17.6527	34.0523	12.4656	24.0463	10.9398	24.3789	35.1634	80.4845

Table 21: RBF model performances - configuration “6“([CDEF])

Number of hidden layer's neurons	RMSE		RRMSE (%)		MAPE (%)		R ² (%)	
	Min	Max	Min	Max	Min	Max	Min	Max
1	38.0202	38.4209	26.8482	27.1312	26.8895	27.2895	7.5527	9.4711
5	32.6269	37.9667	23.0397	26.8104	21.3262	26.9875	10.2609	33.3340
10	26.8921	37.0359	18.9900	26.1532	16.5235	25.5196	15.7530	54.7649
20	17.7372	33.7689	12.5253	23.8462	11.0049	23.1871	33.3877	80.2981
30	17.5991	29.8726	12.4277	21.0947	10.8918	19.5871	45.1169	80.6028
40	17.0345	27.0497	12.0290	19.1013	10.4426	16.7124	54.1802	81.8274
60	16.8767	17.8646	11.9176	12.6152	10.2538	10.9487	80.0512	82.1626
70	16.8584	17.3941	11.9047	12.2830	10.2237	10.7158	81.0521	82.2014
80	16.8461	17.0753	11.8960	12.0579	10.1903	10.4728	81.7402	82.2271
90*	16.8458	17.0167	11.8958	12.0165	10.1836	10.4318	81.8653	82.2277
100	16.8458	17.0290	11.8958	12.0251	10.1837	10.4309	81.8391	82.2277

Table 22: RBF model performances - configuration “7“([ABC])

Number of hidden layer's neurons	RMSE		RRMSE (%)		MAPE (%)		R ² (%)	
	Min	Max	Min	Max	Min	Max	Min	Max
1	39.7218	39.7220	28.0498	28.0500	28.3489	28.3611	1.1857	1.1871
5	39.5331	39.7000	27.9165	28.0344	28.2136	28.3512	1.2982	2.1307
10	39.4453	39.6578	27.8545	28.0046	28.1391	28.3171	1.5047	2.5739
20	39.2557	39.5098	27.7207	27.9001	27.9959	28.2286	2.2946	3.4919
30	39.0835	39.4320	27.5991	27.8451	27.8232	28.1373	2.6764	4.3364
40	39.1279	39.3841	27.6304	27.8113	27.9017	28.1031	2.8598	4.1294
60	38.9472	39.3512	27.5028	27.7881	27.7199	28.0643	3.0216	5.0039
70	38.9052	39.3392	27.4732	27.7796	72.6856	28.0559	3.0809	5.2074
80	38.9166	39.3305	27.4812	27.7735	27.6943	28.0555	3.1239	5.1518
90*	38.9072	39.3027	27.4746	27.7539	27.6756	28.0227	3.2607	5.1978
100	38.9414	39.2545	27.4988	27.7198	27.7165	27.9894	3.4986	5.0309

Table 23: RBF model performances - configuration “8“([ABDEF])

Number of hidden layer's neurons	RMSE		RRMSE (%)		MAPE (%)		R ² (%)	
	Min	Max	Min	Max	Min	Max	Min	Max
1	38.2633	38.3397	27.0199	27.0738	27.0862	27.2647	7.9432	8.3102
5	35.0354	38.3900	24.7405	27.1093	23.7948	27.6656	8.4293	23.1920
10	28.9634	38.1964	20.4527	26.9726	18.2433	27.4758	9.2789	47.4839
20	17.7155	36.3452	12.5099	25.6654	10.9997	25.5622	18.4913	80.3454
30	17.6504	35.4107	12.4640	25.0055	10.9325	24.6804	23.7424	80.4896
40	17.6294	35.4063	12.4491	25.0024	10.9317	24.6629	23.7393	80.6303
60	17.4897	35.3824	12.3504	24.9855	10.7973	24.6498	23.8790	80.8507
70	17.4694	35.3791	12.3361	24.9832	01.7561	24.6569	23.9429	80.8879
80	17.3842	35.1310	12.2760	24.8080	10.6943	24.4327	25.2897	81.0740
90	17.3553	35.1295	12.2556	24.8070	10.6891	24.4324	25.3046	81.1366
100*	17.2837	35.1292	12.2050	24.8067	10.6236	24.4320	25.3068	81.2918

Table 24: RBF model performances - configuration “9“([ACDEF])

Number of hidden layer's neurons	RMSE		RRMSE (%)		MAPE (%)		R ² (%)	
	Min	Max	Min	Max	Min	Max	Min	Max
1	38.2338	38.4188	26.9990	27.1297	27.1649	27.2678	7.5635	8.4511
5	36.1474	38.2019	25.5257	26.9766	24.9798	27.1738	8.6431	18.1998
10	24.3780	37.9172	17.2147	26.7755	15.0143	27.1506	10.4479	62.9360
20	17.6747	36.2536	12.4811	25.6007	11.0294	25.5034	18.2656	80.4381
30	17.5805	35.8421	12.4146	25.3101	10.9481	25.1041	20.9209	80.6462
40	17.5779	35.7041	12.4128	25.2127	10.9436	24.9672	21.6128	80.6511
60	17.1201	35.5734	12.0894	25.1204	10.4494	25.0114	23.2970	81.6453
70	17.0952	35.5735	12.0719	25.1205	10.5287	25.0114	23.2961	81.7017
80	17.0705	35.4409	12.0545	25.0268	10.4671	24.8856	24.1430	81.7506
90	17.0901	35.3332	12.0683	24.9508	10.4745	24.8025	24.6722	81.7088
100*	16.8500	34.8153	11.8988	24.5851	10.2943	24.2634	26.8820	82.2189

Table 25: RBF model performances - configuration “10“([BCDEF])

Number of hidden layer's neurons	RMSE		RRMSE (%)		MAPE (%)		R ² (%)	
	Min	Max	Min	Max	Min	Max	Min	Max
1	38.1214	38.3834	26.9197	27.1047	27.0808	27.2737	7.7335	8.9884
5	35.4153	38.1038	25.0087	26.9072	24.4554	27.0569	9.1179	21.5318
10	25.5587	37.0379	18.0485	26.1546	16.0707	26.1716	14.6060	59.1426
20	17.5624	37.1505	12.4018	26.2341	10.9479	25.9610	13.8615	80.6836
30	17.4257	34.9818	12.3053	24.7027	10.8111	24.2677	26.0226	80.9831
40	17.3477	34.9483	12.2502	24.6790	10.7038	24.2449	26.3379	81.1531
60	17.2889	31.8234	12.2087	22.4723	10.6294	21.4323	39.3937	81.2807
70	17.2424	29.8436	12.1758	21.0743	10.6096	20.0253	48.4356	81.3812
80	17.1304	25.7503	12.0968	18.1838	10.5596	16.7214	61.5906	81.6250
90	16.9911	23.6708	11.9984	16.7153	10.4407	15.1949	67.2353	81.9218
100*	16.9066	22.7580	11.9387	16.0707	10.3229	14.5995	69.9711	82.1002

Table 26: RBF model performances - configuration “11“([ABCDEF])

Number of hidden layer's neurons	RMSE		RRMSE (%)		MAPE (%)		R ² (%)	
	Min	Max	Min	Max	Min	Max	Min	Max
11	38.3170	38.4172	27.0578	27.1286	27.2448	27.2591	7.5713	8.0523
5	37.1383	38.4046	26.2255	27.1196	26.3282	27.2827	7.6384	14.0407
10	30.4519	38.0802	21.5038	26.8906	19.6782	26.9976	9.2039	42.6514
20	18.5955	36.9332	13.1313	26.0806	11.7235	26.3750	16.5543	78.3470
30	17.4526	36.9037	12.3243	26.0598	10.7283	26.3515	16.7034	80.9246
40	17.4295	36.6966	12.3080	25.9136	10.7194	26.1999	18.2240	80.9751
60	17.4142	36.5424	12.2972	25.8046	10.7299	26.0771	19.2036	81.0081
70	17.3290	36.5430	12.2370	25.8051	10.6317	26.0772	19.2000	81.1936
80	17.2972	36.5257	12.2145	25.7929	10.6158	26.0745	19.4203	81.2822
90	17.2686	35.6775	12.1943	25.1939	10.5926	25.4357	25.4690	81.3244
100*	17.2319	35.6744	12.1684	25.1917	10.5937	25.4278	25.2704	81.4038

Table 27: Summary of performances of both models

Model	Number of hidden layer's neurons	RMSE		RRMSE (%)		MAPE (%)		R ² (%)	
		Min	Max	Min	Max	Min	Max	Min	Max
MLP 1	80	39.4579	39.4812	27.8635	27.8799	28.0635	28.2730	2.3864	2.4955
2	70	39.4228	39.4416	27.8387	27.8519	28.1111	28.2423	2.5781	2.6712
3	40	17.4412	17.4561	12.3162	12.3268	10.7430	10.7881	80.9170	80.9495
4	70	39.4527	39.4688	27.8598	27.8711	28.0220	28.2038	2.4429	2.5292
5	70	17.6568	17.7824	12.4685	12.5571	10.9292	10.9960	80.1969	80.4757
6	100	16.8572	16.8701	11.9039	11.9129	10.1833	10.2210	82.1777	82.2055
7	70	38.9510	39.0063	27.5055	27.5446	27.6195	27.7830	4.7271	4.9850
5	70	17.6568	17.7824	12.4685	12.5571	10.9292	10.9960	80.1969	80.4757
8	60	17.2371	17.3641	12.1721	12.2618	10.5625	10.6200	81.1186	81.3949
9	100	16.7465	16.7860	11.8257	11.8536	10.1005	10.1583	82.3541	82.4367
10	40	16.7759	17.0410	11.8464	12.0336	10.1469	10.5324	81.8225	82.3784
11*	70*	16.7208	16.9969	11.8075	12.0025	10.1373	10.4131	81.9100	82.4912
RBF 1	90	39.4513	39.4593	27.8588	27.8645	28.1388	28.1474	2.4881	2.5275
2	80	39.4131	39.5789	27.8318	27.9489	28.1586	28.3248	1.9281	2.7164
3	70	17.4350	17.4350	12.3118	12.3118	10.7608	10.7608	80.9628	80.9628
4	100	39.4387	39.4864	27.8499	27.8836	28.1417	28.1789	2.3542	2.5901
5	90	17.6527	33.8514	12.4656	23.9044	10.9398	23.9074	34.7432	80.4845
6	90	16.8458	17.0167	11.8958	12.0165	10.1836	10.4318	81.8653	82.2277
7	90	38.9072	39.3027	27.4746	27.7539	27.6756	28.0227	3.2607	5.1978
8	100	17.2837	35.1292	12.2050	24.8067	10.6236	24.4320	25.3068	81.2918
9	100	16.8500	34.8153	11.8988	24.5851	10.2943	24.2634	26.8820	82.2189
10*	100*	16.9066	22.7580	11.9387	16.0707	10.3229	14.5995	69.9711	82.1002
11	100	17.2319	35.6744	12.1684	25.1917	10.5937	25.4278	25.2704	81.4038

Table 28: Best performances of both models

Model	Number of hidden layer's neurons	RMSE		RRMSE (%)		MAPE (%)		R^2 (%)	
		Min	Max	Min	Max	Min	Max	Min	Max
MLP 11*	70	16.7208	16.9969	11.8075	12.0025	10.1373	10.4131	81.9100	82.4912
RBF 10	100	16.9066	22.7580	11.9387	16.0707	10.3229	14.5995	69.9711	82.1002

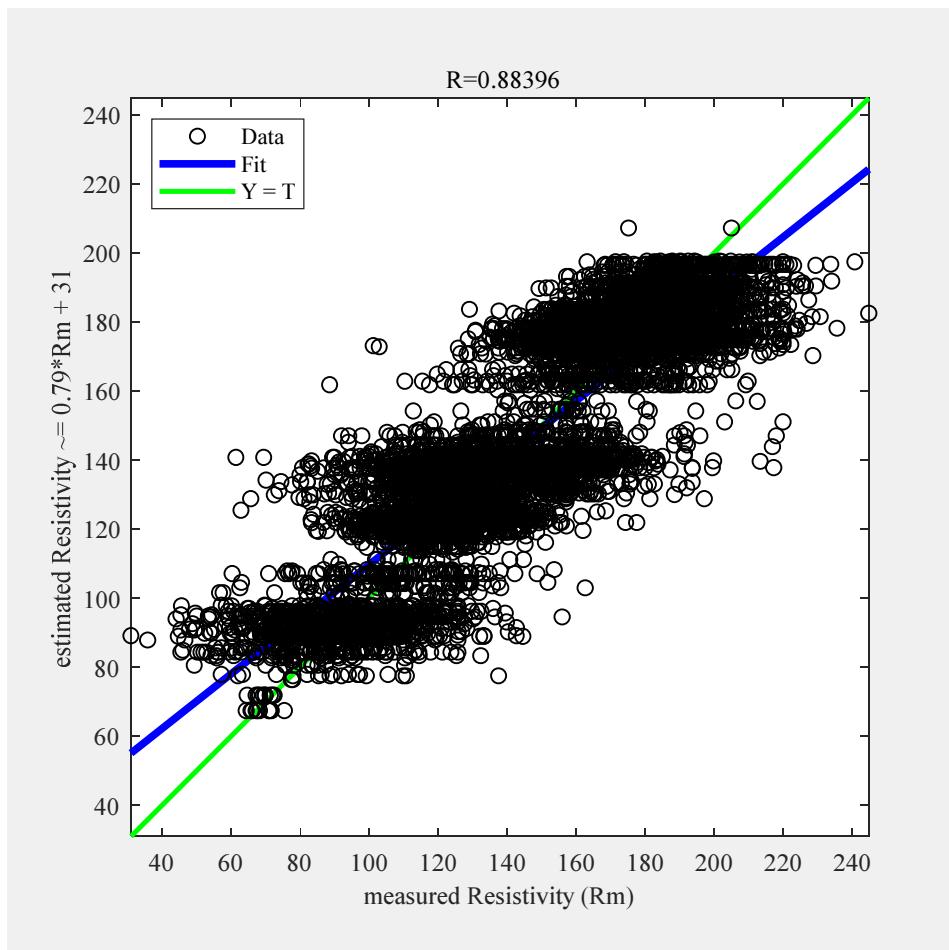


Fig. 14: Correlation between measured and predicted values of soil electrical resistivity

The results obtained for the estimation show that the number of neurons under the hidden layer has a significant impact on the performance of layered networks.

Table 28 shows the most appropriate configuration for modeling the electrical resistivity of the soil. Configuration 11 of the MLP model provides the smallest RRMSE (12.00%) with 70 neurons under the hidden layer.

It should be noted that the number of neurons of the hidden layer and the RRMSE error are the criteria used to select the performance configuration. In view of this work, if you have to choose a model to predict the electrical resistivity of the ground, it must be the MLP 11. Fig.14 shows a correlation between predicted and measured values. With the cloud of points, it is clear that it may

happen that some predictions do not give good results given that some points are too far from the line Y = X (of the first bisector). There is an advantage, however, that the majority of the points are distributed around the right. An enlargement of the database and/or an increase in the number of input parameters may make it possible to overcome this insufficiency.

Conclusion

This work applied artificial neural networks to model the electrical resistivity of soils, based on experimental data collected from nine sites in Lomé. The results show that Perceptron Multilayer configuration (MLP) has the best result compared to the Radial Basis Function (RBF).

This MLP configuration using 70 neurons from the hidden layer predicts the electrical resistivity of the soil with an absolute mean error (MAPE) of 10.41%, a relative mean square error (RRMSE) of 12.00% and R^2 of 81.91%. Thus, by using meteorological parameters (state of nature during and before the day of the measurement, the ambient temperature at the measurement point) and geo-referenced coordinates (longitude, latitude, altitude), we can predict the electrical resistivity of the soil.

Before ended this paper, it should be noted that, speaking of the water content, the more water there is in a material, the more support there is for the ionic movement and therefore the greater its conductivity. For temperatures above the freezing point of water, a decrease in temperature increases the viscosity of the water. This induces a decrease in the mobility of the ions dissolved there in, which causes a decrease in the conductivity and therefore an increase in the resistivity. If the temperature goes below the freezing point of water, there is a sharp decrease in the effective porosity of the soil, which causes a very significant decrease in conductivity. In other way, the surface of the leaflets that make up the clay is generally negatively charged. This structure has natural imperfections and therefore ions are likely to be adsorbed on the faces of the sheets of the clay. When the clay is found in the presence of water, the conduction is greatly facilitated by ion exchange between the water and the surface of the colloids. For any material, the presence of clay increases its electrical conductivity.

Acknowledgement

We would like to express our gratitude to ENSI for its technical supports and University of Lome for lab-facility. Also, we do not forget the reviewers for their valuable comment and those who contributed to the achievement of this work.

Author's Contributions

Kpomonè Komla Apaloo-Bara: He proposed the idea concerning the short term forecasting and participated to the data collection and modeling.

Salami Adekunlé Akim: He reviewed the work and placed it into the research context, including the abstract and conclusion. Also, he contributed to the critical analysis of the obtained results.

Mawugno Koffi Kodjo: He suggested the use of the use of two algorithms. He contributed to write the methodological modeling and data analysis.

Agbassou Guenoukpati: He contributed in drafting article.

Sangué Oraléou Djandja: He contributed for data acquisition.

Koffi-Sa Bedja: He evaluated the pertinence of the topic and approved the status.

Ethics

This article is original and contains unpublished material. All authors declare and attest to no conflicts of interest in relation to this study.

References

- Abda, Z., M. Chittih and B. Zerouali, 2015. Modeling extreme flows by artificial neural networks and neuro-fuzzy inference systems (application to Algiers coastal basins). Proceedings of the International Conference on African Large Basin Hydrology River Hammamet, Oct. 26-30th, Tunisia.
- Afa, J.T. and C.M. Anaele, 2010. Seasonal variation of soil resistivity and soil temperature in Bayelsa State. Am. J. Eng. Applied Sci., 3: 704-709.
- Akim Salami, A., K. Dotche and K.S. Bedja, 2018. Electrical load forecasting using artificial neural network: The case study of the grid Inter-Connected Network of Benin Electricity Community (CEB). Am. J. Eng. Applied Sci., 11: 471-481.
- Anbazhagan, S., 2015. Athens seasonal variation of ground resistance prediction using neural networks. ICTACT J. Soft Comput., 6: 1113-1116.
- Asimakopoulou, F.E., 2011. Artificial neural network approach on the seasonal variation of soil resistance. Proceedings of the 7th Asia-Pacific International Conference on Dans Lightning (APL), pp: 794-799.
- Asimakopoulou, F.E., 2013. Estimation of seasonal variation of ground resistance using Artificial Neural Networks. Electric Power Systems Res., 94: 113-121.
- Choi, J.H. and B.H. Lee, 2012. An analysis of conventional grounding impedance based on the impulsive current distribution of a horizontal electrode. Elsevier.
- Dharmadasa, I.T., 2013. Determination of one dimensional earth resistivity profile in multilayer soil. Engineering Research Unit (ERU & MERcon).
- Gronarz, T., M. Habermehl and R. Kneer, 2016. Modeling of particle radiation interaction in solid fuel combustion with artificial neural networks. J. Power Technologies, 96: 206-211.
- Houndedako, S., 2014. Choice of the configuration of a spike type earth connection for optimal protection. Review of CAMES.
- Kamel, R.M., 2011. Comparison the Performances of three earthing systems for micro-grid protection during the grid connected mode. Int. J. Sustainable Energy.
- Legrand, X., 2007. Modeling of grounding systems for power lines subjected to lightning transients. Ecully, Ecole centrale de Lyon.
- Marcin, G. and P. Furmanski, 2013. Predicting the effective thermal conductivity of dry granular media using artificial neural networks. J. Power Technologies, 93: 59-66.

- Nassereddine, M., R. Jamal and N. Ghalia, 2013. Soil resistivity data computations: Single and two-layer soil resistivity structure and its implication on Earthing design. Int. J. Electrical, Electronic Sci. Eng.
- Nzuru Nsekere, J.P., 2014. Contribution to the analysis and implementation of grounding of electrical installations in tropical regions. Phd Thesis, University of Liège. France.
- Wenner, F., 1915. A method for measuring earth resistivity. J. Washington Academy Sci., 5: 561-563.